

## A CONSTANT TEMPERATURE OPERATION THERMORESISTIVE SIGMA-DELTA SOLAR RADIOMETER

Amauri Oliveira<sup>1</sup>, Lígia S. Palma<sup>1</sup>, Alexandre S. Costa<sup>1</sup>, Raimundo C. S. Freire<sup>2</sup> and Antônio C. C. Lima<sup>1</sup>

<sup>1</sup>Polytechnic School, Federal University of Bahia, Salvador, Brazil

<sup>2</sup> Science and Technology Center, Federal University of Campina Grande, Campina Grande, Brazil

**Abstract** – In this paper we propose a feedback system, with thermo-resistive sensor, based on sigma-delta modulation. The system uses a one-bit sigma-delta modulator in which considerable part of conversion functions is performed by a thermoresistive sensor. The sensor is modelled using the power balance principle and the applied measurement method is constant temperature. This transducer architecture is able to realize digital measurement of physical quantities that interacts with the sensor: temperature, thermal radiation and fluid velocity. This paper presents simulations results of this system applied to thermal radiation measurement.

**Keywords** Thermoresistive sensor, measurement, sigma-delta modulation.

### 1. INTRODUCTION

Negative feedback system configurations with thermoresistive sensor using the power balance principle have been employed in measurement of thermal radiation,  $H$  [1-2], fluid velocity,  $U$  [3-5], and temperature,  $T_a$ , [6]. In the most used method, called constant temperature, the sensor is heated by Joule effect to a chosen temperature and the thermal radiation (or fluid velocity, or temperature) variation is compensated by a change in electrical heating due to the negative feedback employed, and the sensor is kept at an almost constant temperature.

Some configurations were studied to implement a measurement system with a sensor heated to a constant temperature. The most usual is the configuration that uses a Wheatstone bridge with the sensor in one of its branches [7]. In that paper, the relation between the output signal and input physical quantity is not a linear one. Another configuration uses a pulse width modulation in the feedback loop, which has the advantage of having a linear relation between output signal and input, in temperature and thermal radiation measurements. In addition, it permits direct input signal conversion to digital voltage [2].

Another attractive possibility is the use of sigma-delta configurations with the sensor being part of the feedback loop. One-bit sigma-delta modulation is already a feedback configuration in which output signal is an oversampled version of the analog input signal [8-9]. Sigma-delta modulator has been employed, in signal processing, to convert an analog quantity to a digital quantity using simple analog

circuitry. Sigma-delta converters are recognized to be robust and high performance A/D converters.

This work presents a solar radiometer architecture composed of a one-bit sigma-delta modulator in which some of its blocks are the thermoresistive sensor itself. In this way, it is possible to obtain a digital oversampled version of the physical quantities. All results presented here were obtained by simulation.

Two thermal sigma-delta systems were simulated using standard signals: step and sine wave, to evaluate the system performance. One has the functional characteristics of a physical system but cannot be implemented on an integrated circuit. The other structure is equivalent to the first one but can be implemented on an integrated circuit.

### 2. PROPOSED SYSTEM

#### 2.1. Problem Definition

The dynamic heat equation for a thermoresistive sensor is expressed by [4-5].

$$\alpha SH + I_s^2 R_s = hS(T_s - T_a) + mc \frac{dT_s}{dt} \quad (1)$$

In (1),  $\alpha SH$  is the incident thermal radiation absorbed by the sensor,  $I_s^2 R_s$  is the electrical power delivered to the sensor,  $h$  is the heat transfer coefficient referred to the sensor surface area  $S$ ,  $T_s$  is the sensor temperature,  $T_a$  is the surrounding temperature (ambient or fluid temperature),  $m$  is the sensor mass,  $c$  is the sensor specific heat and  $\alpha$  is the sensor transmission heat coefficient. The sensor temperature,  $T_s$ , can be given by:

$$T_s(t) = \int_{-\infty}^t \frac{1}{mc} [\alpha SH(\tau) + R_s(\tau) I_s^2(\tau) + hS(T_a(\tau) - T_s(\tau))] d\tau \quad (2)$$

The block diagram of a first order sigma-delta modulator is shown in Fig. 1. The summation and integration blocks are evidenced to show the similarity with (2).

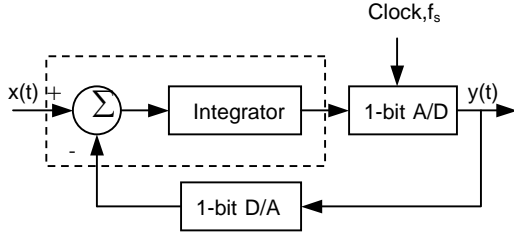


Fig. 1. 1-bit, first order sigma-delta modulator block diagram.

The idea of including the sensor into an one-bit, first order sigma-delta loop becomes from the similarity mentioned and from the fact that the sensor temperature response curve leads to an almost exponential function in response to a square current step for steps of small amplitudes. If the sample frequency,  $f_s$ , is much greater than the sensor linear transfer function pole, this exponential can be approximated by an integration function in which the gain is the exponential function initial slope. The resulting structure can be used to estimate the incident radiation,  $H$ , fluid velocity,  $U$ , or environment temperature,  $T_a$ , according to the case.

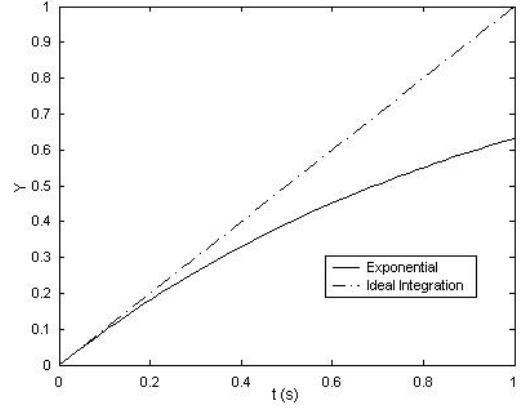


Fig. 2. Step response: ideal integration and exponential.

Fig. 2 shows, for a time constant equal to 1 s, that the step response for an ideal integration, and for the exponential are almost coincident until 10% of this time constant. Based on this fact the transducer model was developed.

This assumption was verified for environment temperature estimation [10]. In that paper,  $h$  was considered constant and  $H$  was considered equal to zero. Here, we present a sigma-delta modulator structure for estimating thermal radiation. In this case,  $T_a$  and  $h$  are considered constant.  $T_s$  can be done by:

$$T_s(t) = \int_{-\infty}^t \frac{1}{mc} (hS(T_a(\tau) - T_s(\tau)) + R_s(\tau) I_s^2(\tau) + \alpha SH(\tau)) d\tau \quad (3)$$

The thermal characteristic for Positive Coefficient Temperature, (PTC) and Negative Coefficient Temperature, (NTC) thermoresistors are given by [4]:

$$\text{PTC: } R_s = R_o [1 + \beta(T_s - T_a)] \quad (4)$$

$$\text{NTC: } R_s = R_o e^{B \left( \frac{1}{T_s} - \frac{1}{T_o} \right)} = A e^{\frac{B}{T_s}} \quad (5)$$

$R_o$  is the sensor resistance at reference temperature  $T_o$ .

## 2.2. Sensor model for small signals

Sensor model for small signals is developed for a PTC sensor heated around equilibrium point ( $T_{so}$ ,  $R_{so}$ ,  $T_{ao}$ ). Small variations of  $T_s$  around this point can be modelled by a tangent straight line taken at this point. The same is valid for NTC sensor [10].

Rewriting (1), considering the substitutions:  $mc$  for  $C_{th}$ ,  $hS$  for  $G_{th}$ ,  $I_s^2$  for  $X_s$  and  $R_s$  for  $R_o(1 + \beta T_s)$  and, including thermal radiation measurement restrictions on  $T_a$  and  $h$ , we obtain:

$$C_{th} \frac{dT_s(t)}{dt} = G_{th} (T_a - T_s(t)) + R_o (1 + \beta T_s(t)) X_s(t) + \alpha SH(t) \quad (6)$$

After linear process and applying Laplace's transform the sensor transfer function is obtained as:

$$T_s(s) = \frac{1}{s - p} [k_x X_s(s) + k_h H(s)] \quad (7)$$

In which  $k_x$ ,  $k_h$  and  $p$  are given by:

$$k_x = \frac{R_{so}}{C_{th}}; \quad k_h = \frac{\alpha S}{C_{th}}$$

and

$$p = \left( \frac{\beta R_o X_{so} - G_{th}}{C_{th}} \right)$$

Sensor square current  $X_{so}$  is given by:

$$X_{so} = \frac{1}{R_{so}} (G_{th} (T_{so} - T_{ao}) - \alpha S H_o) \quad (8)$$

If sensor temperature is kept almost constant,  $H$  can be evaluated from sensor square current knowledge.

$$H = \frac{1}{\alpha S} (G_{th} (T_{so} - T_{ao}) - R_{so} X_s) \quad (9)$$

Fig. 3 shows the PTC sensor model used as a component in the continuous current system of the proposed solar radiometer and this model represents (3). Thermal radiation  $H$  and sensor square current  $I_s^2$  are the input signals and sensor temperature  $T_s$  is the output signal.

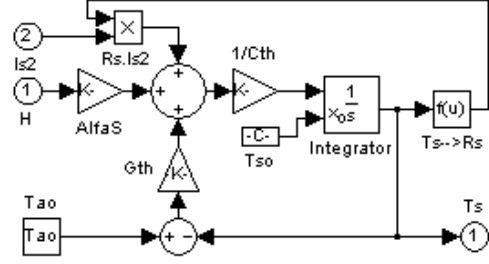


Fig. 3. Block diagram of PTC sensor model

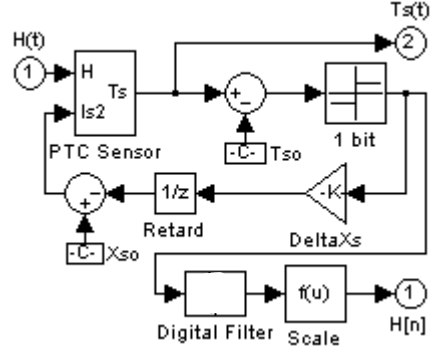


Fig. 4. Continuous current transducer model

### 2.3. Continuous Current Transducer Model

Fig. 4 shows the block diagram for the system in which  $X_s$  is the sensor square current,  $I_s^2$ ,  $T_s(t)$  is the controlled variable and  $H(t)$  is the measurand (thermal radiation).  $T_{so}$  and  $X_{so}$  are the sensor temperature and the sensor square current, respectively, in thermal equilibrium. Current gain is obtained from (8) with  $H_{max}$  and  $H_{min}$  being respectively the full and the bottom scale of solar radiation.

$$\Delta X_s = \frac{\alpha S}{R_{so}} \left( \frac{H_{max} - H_{min}}{2} \right) \quad (10)$$

Two changes must be performed in transducer continuous current model of Fig. 4 to obtain a transducer model that could be implemented on a chip. This is necessary for two reasons: a) first because the sensor model input is a square current; b) second because the quantizer input is a thermal signal and must be changed to an electrical signal.

### 2.4. Pulsed Current Transducer Model

To obtain this model, we first substitute sensor square current,  $I_s^2$ , for a pulse width modulated current, which square rms value is given by [2]:

$$I_{srms}^2 = I_m^2 \frac{\Delta_T}{T_{PWM}} \quad (11)$$

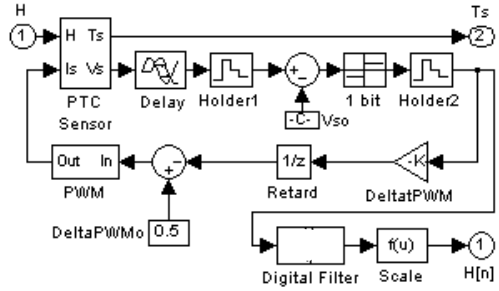


Fig. 5 . Pulsed current transducer model

$I_m$ ,  $\Delta_T$  and  $T_{PWM}$  are respectively, pulse amplitude, pulse width and pulse width modulator (PWM) period. In the pulsed current model,  $I_s^2$  is substituted by the pulse width modulator input, Fig. 5, proportional to  $\Delta_T$  and  $I_{srms}^2$ . This is a special PWM which generates only two pulse widths, one pulse width for quantizer output equal to +1 and another pulse width for quantizer output equal to -1. Pulse width, in equilibrium point, has theoretical value equal to 50 % of PWM period. The information of current gain is now in the pulse width, which has a linear relationship with the solar radiation.

$$\frac{\Delta_T}{T_{PWM}} = \frac{\alpha S}{R_{so} I_m^2} \frac{H_{max} - H_{min}}{2} \quad (12)$$

Second we substitute sensor model output,  $T_s(t)$ , for sensor voltage,  $V_s(t)$ .

Fig. 5 shows pulsed current transducer model, a modified version of continuous current transducer

model including a PWM, and a holder to sample the voltage during current pulse. The sampled voltage between sensor terminals, in equilibrium condition, is given by:

$$V_{so} = R_{so} I_m \quad (13)$$

If  $V_{so}$  is kept constant by the feedback loop,  $R_s$  is also constant and therefore, the sensor temperature too. The transport delay is included, only in simulation, to guarantee the sampling during PWM current pulse.

#### 2.4 Results

The PTC sensor characteristics used to test both systems were:  $\beta = 0,00385 \text{ } ^\circ\text{C}^{-1}$ ,  $R_o = 102,48 \text{ } \Omega$ ,  $G_{th} = 2,982 \times 10^{-3} \text{ W}/^\circ\text{C}$ ,  $C_{th} = 43,06 \times 10^{-3} \text{ J}/^\circ\text{C}$ ,  $S = 20 \times 10^{-6} \text{ m}^2$ ,  $\alpha = 0,95$ .

For both system characteristics:  $T_{so} = 50 \text{ } ^\circ\text{C}$ ,  $T_s(t=0) = 24 \text{ } ^\circ\text{C}$ ,  $H_{min} = 50 \text{ W}/\text{m}^2$ ,  $H_{max} = 1550 \text{ W}/\text{m}^2$ ,  $T_{ao} = 24 \text{ } ^\circ\text{C}$ ,  $R_{so} = 122,21 \text{ } \Omega$ ,  $p = 64,58 \times 10^{-3} \text{ rad/s}$ ,  $f_B = 10.(p/2\pi) = 1,028 \times 10^{-1} \text{ Hz}$ , *Over Sampling Rate (OSR) = 256*,  $fs \geq 2.f_B.OSR = 80 \text{ Hz}$ .

The continuous current model characteristics were:  $X_{so} = 510,05 \times 10^{-6} \text{ A}^2$ ,  $currentgain = 116,6 \times 10^{-6} \text{ A}^2$ .

The pulsed current model characteristics were:  $I_m = 31,94 \text{ mA}$ ,  $T_{PWM} = 1/f_s = 0,0125 \text{ s}$ ,  $widthPWM_o = 0.5 \times T_{PWM}$ ,  $widthgain = 0,1143 \times T_{PWM}$ .

A solar radiation step degree from  $800 \text{ W}/\text{m}^2$  to  $1400 \text{ W}/\text{m}^2$  was applied to the input of continuous current system and to the input of the pulsed current system at  $t=300 \text{ s}$ . The output sensor temperature,  $T_s$ , and the estimated solar radiation,  $H[n]$ , were observed in both systems. Fig. 6 and Fig. 7 show that sensor temperature quickly gets around  $50 \text{ } ^\circ\text{C}$  and remains surrounding this temperature value.

The detail, in Fig. 8 and Fig. 9, shows that this variation remains between  $49,99 \text{ } ^\circ\text{C}$  and  $50,015 \text{ } ^\circ\text{C}$  in continuous current system. In the pulsed current system this variation remains between  $49,985 \text{ } ^\circ\text{C}$  and  $50,02 \text{ } ^\circ\text{C}$ . This variation depends on input solar radiation amplitude and system resolution.

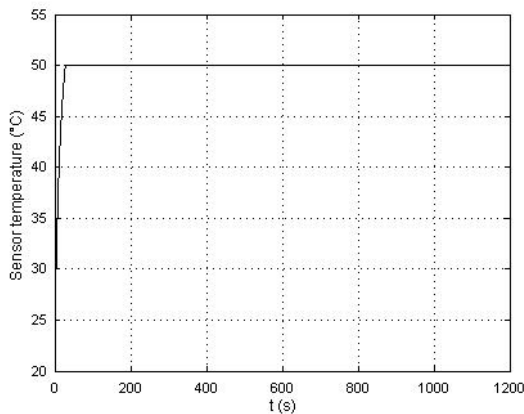


Fig. 6. Continuous current (CC) model: Sensor temperature response to a step of solar radiation at 300 s.

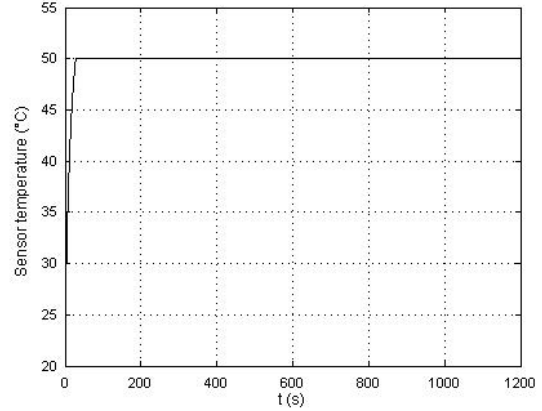


Fig. 7. Pulsed current (PC) model: Sensor temperature response to a step of solar radiation at 300 s.

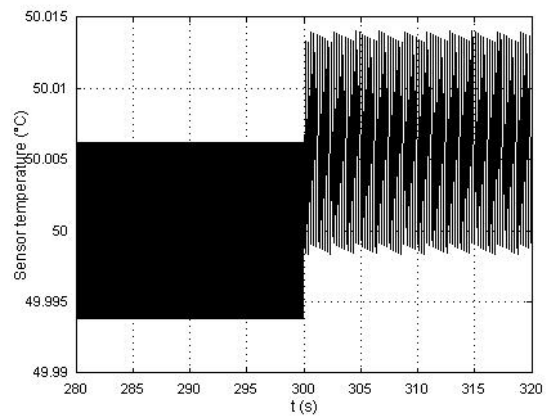


Fig.8. CC model: Sensor temperature response detail to a step of solar radiation at 300 s.

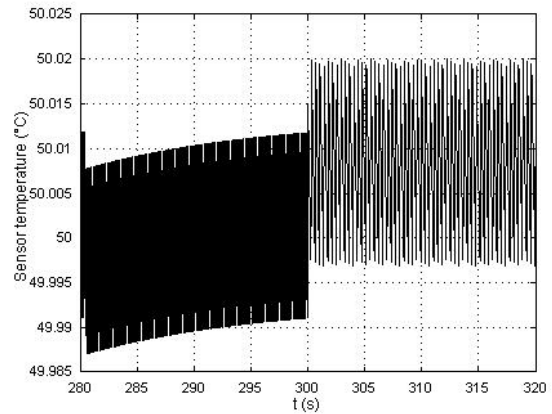


Fig. 9. PC model: Sensor temperature response detail to a step of solar radiation at 300 s.

Fig. 10 and Fig. 11 shows estimated solar radiation for the continuous current system and for the pulsed current system, respectively. The average value of solar radiation begins at  $800 \text{ W}/\text{m}^2$  and moves to nearly  $1400 \text{ W}/\text{m}^2$  after the step time.

Detail of estimated thermal radiation for both systems, after output stabilization, can be seen in Fig. 12. This two values are very close.

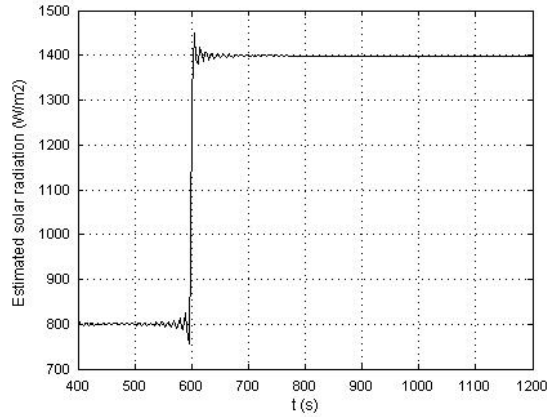


Fig. 10. CC model: Estimated solar radiation, response to a step of solar radiation at 300 s.

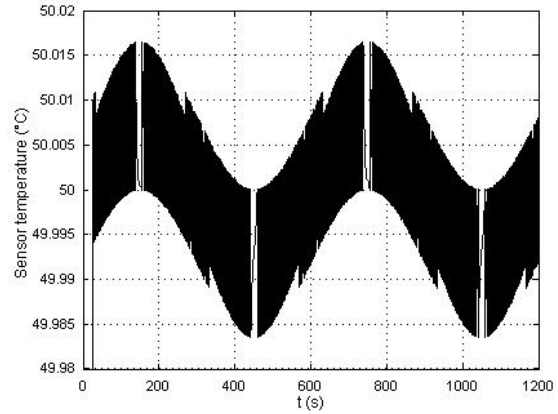


Fig. 13. PC model: Sensor temperature response detail to a sine wave of solar radiation.

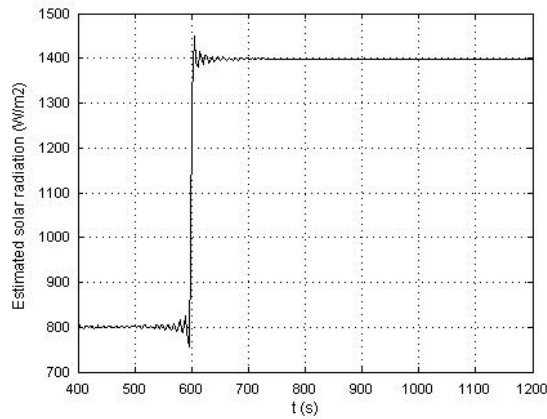


Fig. 11. PC model: solar radiation, response to a step of solar radiation at 300 s

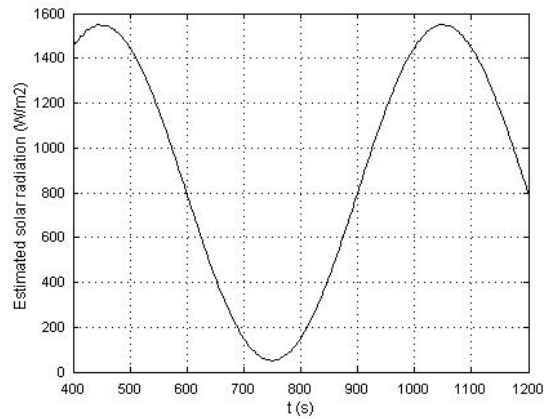


Fig. 14. PC model: Estimated solar radiation, response to a sine wave of solar radiation.

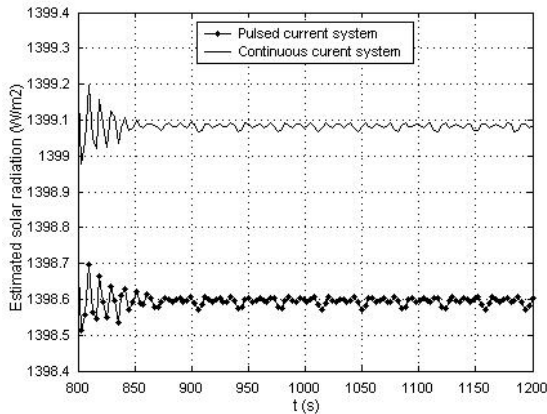


Fig. 12. Both system estimated solar radiation response detail after output stabilization.

Solar radiation value for continuous current system remains surrounding  $1399,1 \text{ W/m}^2$ , with better resolution than pulsed current system, which solar radiation value remains surrounding  $1398,6 \text{ W/m}^2$ .

A sine wave of solar radiation equal to  $H(t) = [800+750\sin(2\pi t/600)] \text{ W/m}^2$  was applied to the pulsed current system input at  $t=0 \text{ s}$  and the outputs (sensor temperature,  $T_s$ , and estimated solar radiation,  $H[n]$ ), were observed.

Fig. 13 shows that sensor temperature is kept around  $50 \text{ }^\circ\text{C}$ , and followed the sine wave input characteristics.

Fig. 14 shows detail of estimated solar radiation corresponding to the input applied to the pulsed current model.

### 3. CONCLUSION

The pulsed current solar radiation architecture presented here as an equivalent system to the continuous current architecture, realized the expected A/D conversion with good resolution when compared to continuous current architecture.

This pulsed current transducer architecture does not need a 1-bit D/A converter in the feedback loop because this function is realized by PWM.

This pulsed current architecture, based on sigma-delta modulation, is well indicated for integrating sensor and circuits on a chip as a microsensor.

This thermal sigma-delta solar radiation, compared to other methods using power balance principle, has the advantage of transforming directly the physical quantity to its corresponding digital value.

The time response of this architecture should still be better analyzed. It is hoped that the systems with

pulsed current have, in the worst case, the same time response of the continuous systems, but with the advantage of directly digital output signal, avoiding errors due to the signal analog processing.

Fluid velocity transducer based in this same principle, will be our future objective.

#### 4. ACKNOWLEDGEMENTS

The authors wish to thank CAPES/Procad and CNPq for financial support and the award of fellowships during investigation period.

#### REFERENCES

- [1] A. Oliveira, G. S. Deep, A. M. N. Lima and R. C. S. Freire, "A Feedback I<sup>2</sup>-Controlled Constant Temperature Solar Radiation Meter". *IEEE-IMTC-1998*, vol. 2, 1998, 1062-1066.
- [2] R. C. S. Freire, G. S. Deep and C. C. Farias, "Electrical Equivalence Solar Radiometer Configurations", *XI Brazilian Automation Congress*, vol. 3, 1996, 1249-1254.  
R. C. S. Freire, G. S. Deep and C. C. Farias, "Configurações de um Radiômetro Solar de Equivalência Elétrica", *XI Congresso Brasileiro de Autômática*, vol. 3, 1996, 1249-1254.
- [3] H. Fujita, T. Ohhashi, M. Asakura, M. Yamada and K. Watanabe, "A Thermistor Anemometer for Low-Flow-Rate Measurements", *IEEE Trans. on Instrum. Meas.*, vol. 44, no 3, 1995, 779-782.
- [4] O. E. Doebelin, "Measurement System Application and Design", Singapore: *McGraw-Hill Book Co*, 4th edition, 1990, cap 7: Flow Measurement.
- [5] R. P. C. Ferreira, R. C. S. Freire, S. G. Deep, J. S. Rocha Neto and A. Oliveira, "Fluid Temperature Compensation in a Hot Wire Anemometer Using a Single Sensor", *IEEE-IMTC-2000*, vol.1, 2000, 512-517.
- [6] L. S. Palma, A. Oliveira, A. S. Costa, A. Q. Andrade Jr, C. V. R. Almeida, M. E. P. V. Zurita and R. C. S. Freire, "Implementation of a Feedback I<sup>2</sup>-Controlled Constant Temperature Environment Temperature Meter", *Sensors*, vol. 3, issue 10, 2003, 498-503, <http://www.mdpi.net/sensors>.
- [7] P. C. Lobo, "An Electrically Compensated Radiometer", *Solar Energy*, vol.36, n° 3, 1985, 207-216.
- [8] H. Inose and Y. Yasuda, "A Unity Bit Coding Method by Negative Feedback", *Procs. of IEEE*, vol. 51, n° 11, 1963, 1524-1535.
- [9] P. M. Aziz, H. V. Sorensen and J. V. D. Spiegel, "An Overview of Sigma-Delta Converters", *IEEE Signal Processing Magazine*, 1996, 61-84.
- [10] A. Oliveira, A. S. Costa, L. S. Palma, R. C. S. Freire and A. C. C. Lima, "A Constant Temperature Operation Thermo-resistive  $\Sigma$ - $\Delta$  Transducer", *IEEE-IMTC-2004*, "in press".

---

**Author(s):** Dr., Amauri Oliveira, Electrical Engineering Department, Polytechnic School, Federal University of Bahia, Rua Aristides Novis 2, CE 40210-630, Salvador, Brazil, Fone: +55 71 2039776, Fax: +55 71 2039779 [amauri@ufba.br](mailto:amauri@ufba.br).

M.Sc., Lúgia Souza Palma, Electrical Engineering Department, Polytechnic School, Federal University of Bahia, Rua Aristides Novis 2, CEP 40210-630, Salvador, Brazil, Fone: +55 71 2039776, Fax: +55 71 2039779, [ligia@ufba.br](mailto:ligia@ufba.br).

B.Sc., Alexandre Santana Costa Electrical Engineering Department, Polytechnic School, Federal University of Bahia, Rua Aristides Novis 2, CEP 40210-630, Salvador, Brazil, Fone: +55 71 2039760, Fax: +55 71 2039779, [ascosta@ufba.br](mailto:ascosta@ufba.br).

Dr., Raimundo Carlos Silvério Freire, Electrical Engineering Department, Science and Technology Center, Federal University of Campina Grande, Av. Aprígio Veloso 882, CEP 58109-970, Campina Grande, Brazil, Fone: +55 83 3101447, Fax: +55 83 3101015, [freire@dee.ufcg.edu.br](mailto:freire@dee.ufcg.edu.br).

Ph.D., Antônio César de Castro Lima, Electrical Engineering Department, Polytechnic School, Federal University of Bahia, Rua Aristides Novis 2, CE 40210-630, Salvador, Brazil, Fone: +55 71 2039760, Fax: +55 71 2039779 [acdcl@ufba.br](mailto:acdcl@ufba.br).